Japanese Journal of Applied Physics **50** (2011) 070110
DOI: 10.1143/JJAP.50.070110

Resistive Switching in Al/Graphene Oxide/Al Structure

Gennady N. Panin[1,2*], Olesya O. Kapitanova[3], Sang Wuk Lee[1], Andrey N. Baranov[4], and Tae Won Kang[1]

[1]*Department of Physics, Quantum-functional Semiconductor Research Center, Dongguk University, Seoul 100-715, Republic of Korea*
[2]*Institute of Microelectronics Technology, RAS, Chernogolovka, Moscow district, 142432, Russia*
[3]*Department of Material Science, Moscow State University, 119992, Moscow, Russia*
[4]*Department of Chemistry, Moscow State University, 119992, Moscow, Russia*

Received December 29, 2010; accepted April 5, 2011; published online July 20, 2011

We report resistive switching behaviors in an Al/graphene oxide/Al planar structure. Graphene oxide was synthesized by a modified Hummer's method from graphite rods. The planar structures were fabricated on a Si/SiO_2 substrate by spin-coating graphene oxide suspensions and patterning Al electrodes by photolithography. Both diode-like (rectifying) and resistor-like (nonrectifying) behaviors were observed in the device switching characteristics. Electrical characterization of the Al/graphene oxide interface using the induced current identified a potential barrier near the interface and its spatial modulation, caused by local changes of resistance at a bias voltage, which correlated well with the resistive switching of the whole structure. The mechanism of the observed local resistance changes near the electrode and the associated resistive switching of the entire structure is associated with the electrodiffusion of oxygen and the formation of sp^2 graphene clusters in an sp^3 insulating graphene oxide layer formed near the electrode by a pre-forming process.

1. Introduction

Thin films of graphene oxide (GO) have recently emerged as a new carbon-based nanoscale material for potential applications in resistive random access memory (RRAM).[1,2] The traditional charge-based memory devices such as dynamic random access memory (DRAM) and flash memory have technological and physical limitations. RRAM, based on a mechanism of change in resistance, has attracted attention as a promising next-generation nonvolatile memory owing to its simple structure, facile processing, high density, high operation speed, long retention time, and low power consumption.[3–5]

The unique mechanical and electronic properties of graphene as a two-dimensional crystal[6] have also led to scrutiny of the properties of its oxide — GO,[7–13] which consists of a single layer of graphene bound to oxygen in the form of carboxyl, hydroxyl, or epoxy groups. GO is a wide band gap material (band gap the order of 6 eV) but a controlled oxidation/reduction process provides tunability of the electronic, optical, and mechanical properties including the possibility of accessing zero-band-gap graphene via complete removal of the C–O bonds. The high solubility of graphene oxide in water and other solvents allows it to be uniformly deposited onto any substrate in the form of thin films using simple methods such as drop-casting, spin coating, Langmuir–Blodgett deposition, and vacuum filtration. This makes it potentially useful for the fabrication of large-scale flexible, transparent, and printable devices.[7]

The transport of charge carriers in reduced GO (r-GO) is limited by the structural disorder. However, the reported conductivity between 0.05 and 2 S/cm and the room-temperature field-effect mobilities of 2–200 $cm^2\,V^{-1}\,s^{-1}$ for holes and 0.5–30 $cm^2\,V^{-1}\,s^{-1}$ for electrons[9] are sufficiently large for applications where inexpensive and moderate performance electronics are required (such as printable electronics on flexible platforms, like tags, etc.). Moreover, the transport in r-GO is intriguing owing to the presence of substantial electronic disorder arising from variable sp^2 and sp^3 carbon ratios. In GO, the majority of carbon atoms bonded with oxygen are sp^3 hybridized, which disrupts the extended sp^2 conjugated network of the original graphene sheet.

Recently, reliable and reproducible resistive switching of GO thin films[14,15] and conjugated-polymer functionalized GO films[16,17] has been reported. However, the microscopic origin of the resistive switching of thin GO films is not fully understood.

Here, we report a resistive switching structure based on a GO thin film in simple geometry with two planar aluminum electrodes and study the mechanism of resistive switching in this structure. An Al/GO film/Al planar device structure was made on Si/SiO_2 substrate with a uniform GO film prepared by spin-coating. This device showed reliable and reproducible unipolar and bipolar resistive switching (URS/BRS) depending on the forming process with an on/off ratio of current $\sim 10^3$ and switching voltages of ~ 0.7 V. The remote electron-beam-induced current (REBIC) measurements used in this work showed that the forming process was accompanied by the formation of the potential barrier near the electrode. Modulation of the barrier by the bias voltage leads to the spatial changes of its resistance and the resistive switching (RS) structure. The microscopic origin of the RS behavior is evident from the detection of conductive filaments in the Al/GO interface layer that arise from the reversible diffusion of negatively charged oxygen ions and the formation of sp^3 and sp^2 clusters upon the set and reset processes, respectively.

2. Experimental Methods

2.1 Preparation of GO

GO was synthesized by oxidation of graphite using the modified Hummer's method,[18,19] in which the long oxidation time was combined with a highly effective method for the purification of reaction products. 2 g of natural graphite (Aldrich graphite, rod, purity 99.995 wt %, high density) and 1.5 g of $NaNO_3$ (purity 99%) were placed in a flask. Then, 124.2 g of H_2SO_4 (purity 96%) was added and the mixture was stirred and cooled in an ice water bath simultaneously. As a result we obtain a mix of graphite and concentrated HNO_3 and H_2SO_4. 15 g of $KMnO_4$ (purity 99%) (as a reducing agent) was gradually added over about 20 min. Cooling was completed in 2 h, and the mixture was allowed

*E-mail address: g_panin@dgu.edu

to stand for 24 h at about room temperature with gentle stirring to obtain a highly viscous liquid. In this step, the interaction of sodium nitrate and sulfuric acid with graphite takes place, which promotes the expansion of the graphite layers (intercalation of sulfuric acid in graphite), and then graphite oxidation is expanded by potassium permanganate. Prolonged exposure of the mixture within 2–3 days not only leads to expansion of graphite and its oxidation, but also to an exfoliation of the oxidized graphite into thin GO flakes. The obtained liquid was added to 200 ml of 5 wt % H_2SO_4 aqueous solution for 20 min with stirring, and the resultant mixture was further stirred for 40 min. Then, 6 g of 30 wt % H_2O_2 aqueous solution was added to the above liquid and the mixture was stirred for 40 min. To remove ions of oxidant origin, especially manganese ions, the resultant liquid was purified by repeating the following procedure cycle 15 times: centrifugation, removal of the supernatant liquid, addition of a mixed aqueous solution of 3 wt % H_2SO_4/0.5 wt % H_2O_2, and shaking to re-disperse. The above purification procedures were similarly repeated a further three times except that the liquid to be added was replaced with water. Multiple washing by the mixture with hydrogen peroxide and then by water is necessary for complete removal of the reaction products. The resultant mixture was allowed to stand for one day, to precipitate thick particles, etc. The precipitated particles were removed, and just one half of the remaining dispersion was purified by repeating the same procedures a further 20 times with water. When the extra small ions derived from oxidants are thoroughly removed by high purity purification, many layers tend to separate automatically from each other owing to interlayer electrostatic repulsion, and then the single-layer GO flakes in aqueous dispersion are formed.

2.2 Reduction of GO

The resulting GO was partially reduced in two ways: 1) by annealing in an Ar/H_2 mixture (90% Ar, 10% H_2) at 900 °C for 15 min and 2) by adding ascorbic acid to suspensions of GO and annealing of the samples at 200 °C in Ar within 12 h.

2.3 Preparation of Al/GO/Al structures and their characterization

The Al/GO/Al planar structures were fabricated on a Si/SiO_2 substrate by using spin-coating GO suspensions to obtain the uniform thin films (50–100 nm) and patterning of electrodes by photolithography (25–50 μm separation). The current–voltage (I–V) characteristics of fabricated Al/GO/Al structures were measured at RT using a Keithley 4200 SCS semiconductor parameter analyzer in voltage sweeping mode. Spatial electrical properties of the structures were characterized using an XL 30SFEG HRSEM with EBIC system. Transmission electron microscope (TEM), selective area electron diffraction (SAED), X-ray diffraction (XRD), atomic force microscopy (AFM), and Raman measurements were used to characterize the GO structure.

3. Results and Discussion

3.1 Characterization of GO structure

The resulting GO was well exfoliated. The flakes were usually a few layers thick and several tens of micrometers in diameter. The thicknesses of GO flakes are usually in the range of 1–1.4 nm. Figure 1 shows a typical AFM image of a single GO flake of 1.1 nm thick. The electron diffraction in TEM (Fig. 2) shows both crystalline and amorphous patterns in different areas of the flakes indicating their spatially inhomogeneous electronic properties. Figure 3 shows the XRD spectrum of a GO thin film. The main XRD peak is attributed to the GO interlayer spacing. The observed weak XRD peaks are characteristic of partially reduced GO.

Raman spectra of graphene oxide, obtained before and after its reduction, show the characteristic D (1357 cm^{-1}) and G (1578 cm^{-1}) peaks (Fig. 4). The appearance of the D band in our samples signifies disorder in the carbon lattice. The intensity ratio of the D and G bands is a measure of the disorder, as expressed by the sp^2/sp^3 carbon ratio.[20] After

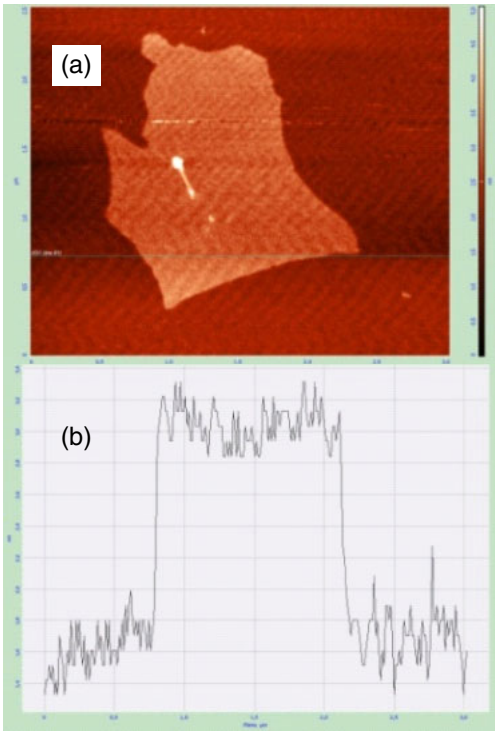

Fig. 1. (Color online) AFM image of a single GO flake and its thickness profile.

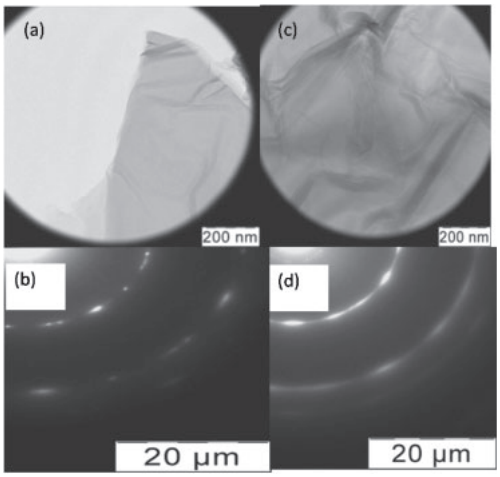

Fig. 2. TEM images (a, c) and SAED patterns (b, d) of a GO single flake obtained at different points.

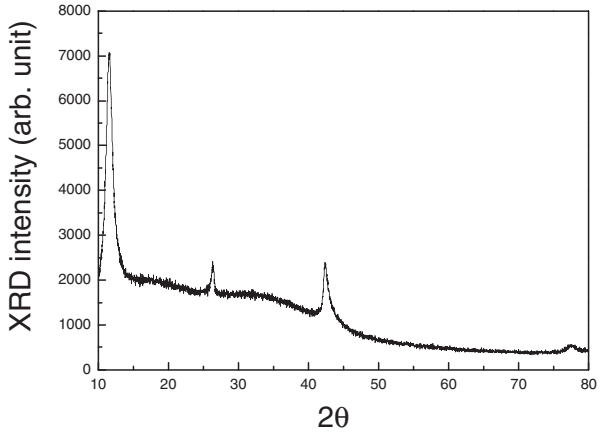

Fig. 3. XRD pattern of the GO film.

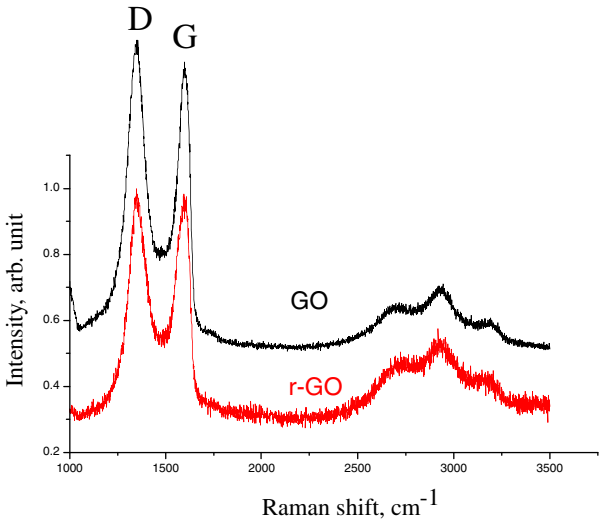

Fig. 4. (Color online) Raman spectra of GO films obtained before (black line) and after (red line) reduction.

the reduction, the ratio of intensities of peaks G to D increases, which can be attributed to a decrease in the density of defects and changes in the ratio of sp^2 and sp^3 clusters.

3.2 Electrical measurements

I–V characteristics of the fabricated structures are shown in Fig. 5. Bias to the structure swept at a constant rate from 0 to 1 V and back from 1 to −1 through 0 and back to zero initial state. *I–V* curves of the structure, which have not been subjected to the forming voltage, showed a linear behavior with no appreciable hysteresis [Fig. 5(a)]. However, the pre-forming of the structure even at low bias voltage (2 V) led to a clear hysteresis *I–V* curve [Fig. 5(b)]. In this case, the soft bipolar resistive switching was observed. With increasing bias stress, we observed the transition of the structure of bipolar ($V = 2$ V) to the unipolar soft switching ($V = 3$ V) [Fig. 5(c)]. For higher forming voltages ($V = 5$ V) the structure showed a sharp unipolar resistive switching [Fig. 6]. The ratio of the on and off currents was about 10^3, and the threshold voltage transition to a low resistive state was in the range of 0.5–1 V, depending on the forming voltage.

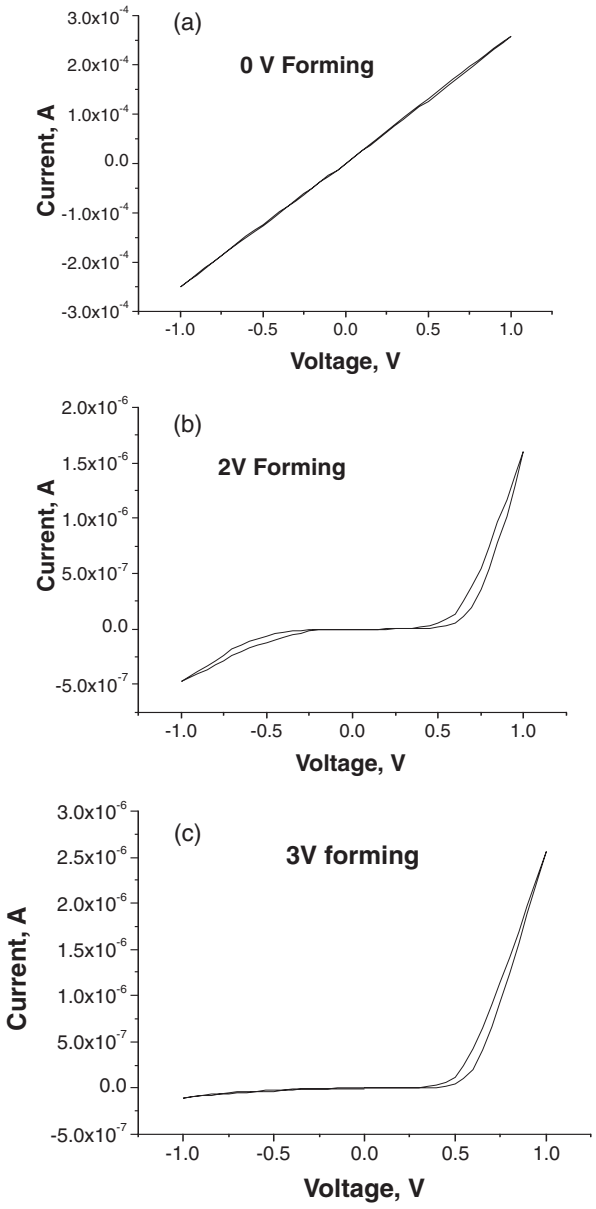

Fig. 5. *I–V* curves of Al/GO/Al structures pre-formed at different forming voltages.

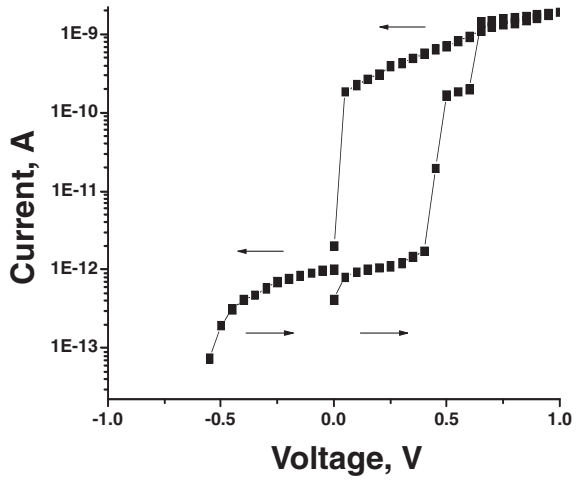

Fig. 6. Resistive switching of the Al/GO/Al structure pre-formed at 5 V.

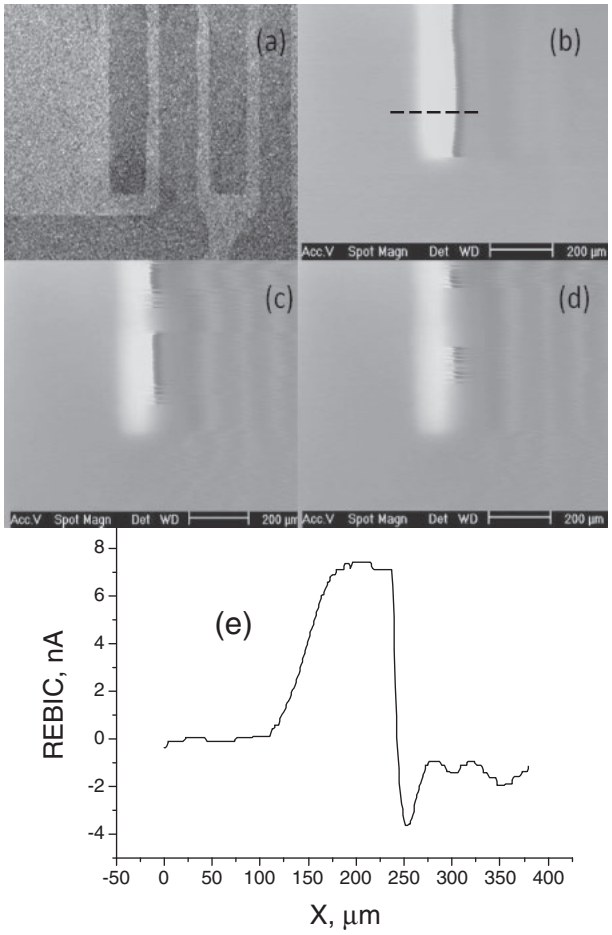

Fig. 7. SEM images of the Al/GO/Al structure in SE (a) and REBIC mode (b) 0, (c) 0.5, and (d) 1 V; (e) REBIC profile obtained by scanning across the Al/GO interface along the dotted line in (b).

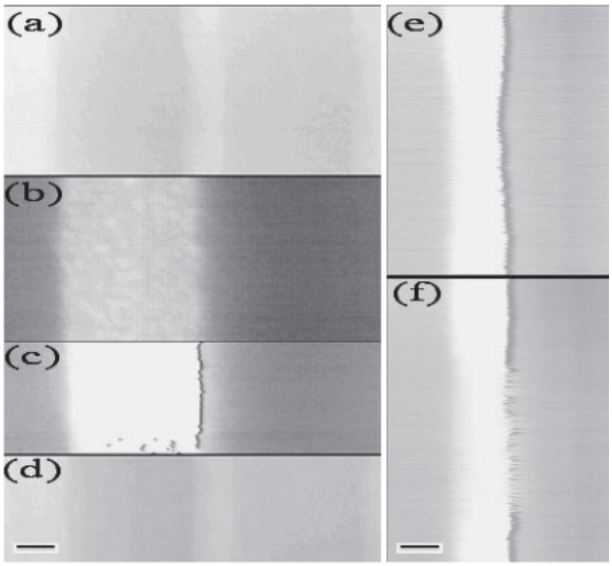

Fig. 8. SEM-REBIC images of the Al/GO/Al structure with the built-in potential barrier modulation near the negatively biased Al electrode at different bias (V_b) and forming (V_f) voltages: (a) $V_b = 0$; $V_f = 0$ (SE mode); (b) $V_b = 0$; $V_f = 0$ (REBIC mode); (c) $V_b = 0$; $V_f = 5$ V (REBIC mode); (d) $V_b = 0$; $V_f = 5$ V (SE mode); (e) $V_b = 0.2$ V; $V_f = 7$ V (REBIC mode); (f) $V_b = 0.5$ V; $V_f = 7$ V [REBIC mode, the same region as in (e)]. Scale bars are 100 µm in (e) and (f), 50 µm in (a)–(d). Images in (a)–(d) were obtained by using sequential switching of detected signals of secondary electrons (SE) and the induced current (REBIC) during the electron beam scanning.

A similar effect of the resistive switching in graphene oxide structures was reported in refs. 14 and 15. However, the mechanism of switching of a high resistance state (HRS) to a low resistance state (LRS) is not fully understood. It was assumed that the electrodiffusion of metal atoms of the electrode can lead to the formation of highly conductive filaments in the bulk oxide film that can switch the structure.[14] In ref. 15 the resistive switching in the Al/GO/Al structure was explained by the formation of conducting filaments of aluminum atoms in a thin interface layer of amorphous aluminum oxide that is formed in the manufacturing process of the upper electrode.

To investigate the mechanism of resistive switching in our Al/GO/Al structure, we used the REBIC technique. This method is widely used to characterize charge transport in semiconductors with built-in potential barriers with a spatial resolution.[21] Figure 7 shows SE (a) and REBIC (b–d) images of the pre-formed (5 V) Al/GO/Al structure before (b) and after (c, d) switching from HRS to LRS as well as the REBIC profile obtained by scanning across the Al/GO interface barrier (e). In the high resistance state ($V < 0.5$ V), an additional potential barrier near the electrode is detected as a narrow continuous line of dark REBIC contrast [Fig. 7(b)]. Applied voltage on the order of 0.5–1 V leads to local breakdowns in the barrier layer, which appear in the REBIC mode owing to a local decrease in the induced current. As a result, a broken line of dark REBIC contrast is detected. [Figs. 7(c) and 7(d)]. In this state, the structure shows a low resistance. A reverse bias restores the high resistance state and the continuous potential barrier near the electrode is detected again in the REBIC mode. The profile of the induced current, obtained by scanning an electron beam across the interface of the structure, shows that a potential barrier with the opposite direction of the electric field (negative current and dark REBIC contrast) is formed near the positively biased electrode [Fig. 7(e)]. Spatial modulation of the current along the barrier is correlated with the applied voltage. Local breakdown of this barrier is apparently responsible for the observed resistive switching. It should be noted that the structure without a forming process, demonstrates only the barriers associated with electrodes that do not show distinguishable features of local breakdown. Figure 8 shows the SEM-REBIC data of the built-in barrier modulation at different bias (V_b) and forming (V_f) voltages. The structure without the forming process shows only a bright-dark contrast of the induced current caused by the electric fields of Schottky contacts [Fig. 8(b)]. However, once this structure was subjected to the forming bias voltage (5 V), a new barrier near the positively biased electrode is detected in the induced current mode as a narrow line of dark REBIC contrast [Figs. 8(c) and 8(e)]. In this state, the structure shows a high resistance, which is characteristic for its HRS. Reverse bias (negative voltage on the electrode) leads to local breakdowns in the barrier layer, which appear as an intermittent narrow line of dark REBIC contrast with the spatially modulated magnitude of the induced current [Fig. 8(f)]. The formation of a potential barrier and its spatial local breakdown are well reproduced

and invertible upon application of the reverse and forward voltages. It should be noted that the higher bias voltage increases the number of local breakdowns, which could be used for multi-state switching.

3.3 Model of resistive switching

REBIC studies with a high spatial resolution indicate that the forming bias leads to the formation of a highly resistive region near the positively biased electrode. Electrodiffusion of oxygen ions to the positively charged electrode could lead to the formation of a continuous sp^3 layer between this electrode and the r-GO layer that accompanies the transition of structure in the high resistance state. The reverse bias voltage, which generates an electric field in the opposite direction, leads to a back diffusion of oxygen and the formation of low resistive filaments in the GO layer near the contact region. Possible rearrangement of the structure owing to the electrodiffusion of excess oxygen in GO at room temperature for quite long distances is in good agreement with the observed rearrangement of the potential barrier at distances of several micrometers from the electrode.

Electrodiffusion of hydrogen and oxygen in graphene devices was reported in refs. 22 and 23, where the effect of adsorption of these atoms from the atmosphere on the switching characteristics of a graphene FET device was investigated. A strong decrease in current flow was observed at high voltages at the second gate, which was attributed to the onset of the insulating state induced by the electrochemical doping, which involves graphene oxidation and was amplified by the transverse electric field. It was also shown that one sp^3 carbon–oxygen or carbon–hydroxyl bond per 10^6 sp^2 bonds decreased the conductivity of CNTs by 50%.[24] The observed switching of the resistance in our structure could be explained by a model of cluster structure of GO consisting of the sp^2 clusters in an sp^3 matrix enriched with oxygen[25] and its local reversible rearrangement near the electrical contact in a high electric field. The forming process leads to the formation near the electrode high potential barrier, which is apparently associated with sp^2–sp^3 phase rearrangement. The negative bias voltage leads to a back diffusion of oxygen and the formation of sp^2 cluster filaments, which leads to the switching structure in the low resistive state (LRS). The reverse bias voltage results in the formation of an isolated sp^3 cluster layer near the electrode and switching in the high resistance state (HRS).

4. Conclusions

Resistive switching was observed in the planar structure of Al/GO/Al at room temperature. Without the pre-forming process, a smooth transition ("soft" switch) of both ohmic bipolar and rectifying unipolar (bipolar) behavior was detected. The reliable forming process leads to the abrupt switching of the structure. Electrical characterization of the Al/graphene oxide interface with high spatial resolution using the induced current technique revealed a potential barrier near the interface and its spatial modulation, caused by local changes of resistance under applied voltages. The local changes of resistance in the layer near the Al/GO interface under a bias voltage as a result of sp^3 to sp^2 structure reconstruction are assumed to be responsible for the observed resistive switching. The mechanism of the resistive switching in the structure is supposed to be related to the electrodiffusion of oxygen and the formation of sp^2 graphene clusters in the sp^3 insulating graphene oxide layer formed near the electrode by a pre-forming process.

Acknowledgments

This work was supported by a National Research Foundation of Korea (NRF) grant funded by the Ministry of Education, Science and Technology (MEST) No. 2011-0000016 as well as by the Leading Foreign Research Institute Recruitment Program through NRF funded by MEST No. 2010-00218, and a Russian Ministry of Science and Education grant No. 02.740.11.5215.

1) R. Waser and M. Aono: Nat. Mater. **6** (2007) 833.
2) D. Strukov, G. Snider, D. Stewart, and R. Williams: Nature **453** (2008) 80.
3) G. I. Meijer: Science **319** (2008) 1625.
4) A. Sawa: Mater. Today **11** [6] (2008) 28.
5) R. Waser, R. Dittmann, G. Staikov, and K. Szot: Adv. Mater. **21** (2009) 2632.
6) K. S. Novoselov, A. K. Geim, S. V. Morozov, D. Jiang, Y. Zhang, S. V. Dubonos, I. V. Grigorieva, and A. A. Firsov: Science **306** (2004) 666.
7) G. Eda, G. Fanchini, and M. Chhowalla: Nat. Nanotechnol. **3** (2008) 270.
8) K. A. Mkhoyan, A. W. Contryman, J. Silcox, D. A. Stewart, G. Eda, C. Mattevi, S. Miller, and M. Chhowalla: Nano Lett. **9** (2009) 1058.
9) C. Gómez-Navarro, R. T. Weitz, A. M. Bittner, M. Scolari, A. Mews, M. Burghard, and K. Kern: Nano Lett. **7** (2007) 3499.
10) G. Eda, Y.-Y. Lin, S. Miller, C.-W. Chen, W.-F. Su, and M. Chhowalla: Appl. Phys. Lett. **92** (2008) 233305.
11) H. A. Becerril, J. Mao, Z. Liu, R. M. Stoltenberg, Z. Bao, and Y. Chen: ACS Nano **2** (2008) 463.
12) J. Wu, H. A. Becerril, Z. Bao, Z. Liu, Y. Chen, and P. Peumans: Appl. Phys. Lett. **92** (2008) 263302.
13) B. C. Brodie: Philos. Trans. R. Soc. London **149** (1859) 249.
14) C. L. He, F. Zhuge, X. F. Zhou, M. Li, G. C. Zhou, Y. W. Liu, J. Z. Wang, B. Chen, W. J. Su, Z. P. Liu, Y. H. Wu, P. Cui, and R.-W. Li: Appl. Phys. Lett. **95** (2009) 232101.
15) H. Y. Jeong, J. Y. Kim, J. W. Kim, J. O. Hwang, J.-E. Kim, J. Y. Lee, T. H. Yoon, B. J. Cho, S. O. Kim, R. S. Ruoff, and S.-Y. Choi: Nano Lett. **10** (2010) 4381.
16) X.-D. Zhuang, Y. Chen, G. Liu, P.-P. Li, C.-X. Zhu, E.-T. Kang, K.-G. Noeh, B. Zhang, J.-H. Zhu, and Y.-X. Li: Adv. Mater. **22** (2010) 1731.
17) G. Liu, X. Zhuang, Y. Chen, B. Zhang, J. Zhu, C.-X. Zhu, K.-G. Neoh, and E.-T. Kang: Appl. Phys. Lett. **95** (2009) 253301.
18) W. Hummers and R. Offeman: J. Am. Chem. Soc. **80** (1958) 1339.
19) M. Hirata, T. Gotou, S. Horiuchi, M. Fujiwara, and M. Ohba: Carbon **42** (2004) 2929.
20) A. C. Ferrari and J. Robertson: Phys. Rev. B **61** (2000) 14095.
21) G. Panin, C. Dıaz-Guerra, and J. Piqueras: Appl. Phys. Lett. **72** (1998) 2129.
22) T. J. Echtermeyer, M. C. Lemme, M. Baus, B. N. Szafranek, A. K. Geim, and H. Kurz: arXiv:0712.2026v1.
23) T. J. Echtermeyer, M. C. Lemme, M. Baus, B. N. Szafranek, A. K. Geim, and H. Kurz: IEEE Electron Device Lett. **29** (2008) 952.
24) B. R. Goldsmith, J. G. Coroneus, V. R. Khalap, A. A. Kane, G. A. Weiss, and P. G. Collins: Science **315** (2007) 77.
25) C. Mattevi, G. Eda, S. Agnoli, S. Miller, K. A. Mkhoyan, O. Celik, D. Mastrogiovanni, G. Granozzi, E. Garfunkel, and M. Chhowalla: Adv. Funct. Mater. **19** (2009) 2577.

Gennady Nikolayevich Panin is currently a professor of Department of Physics, the Quantum-functional Semiconductor Research Center (QSRC) at Dongguk University and a senior scientist at the Institute of Microelectronics Technology, Russian Academy of Sciences (IMT RAS). He graduated from Moscow National University (State Institute of Electronic Technology) in applied physics and electronics, with honors, and received his doctorate in physics of semiconductors and solid state electronics from IMT RAS in 1994. He worked as a visiting scientist at the Institute of Solid State Physics, Halle, Germany in 1986 and the Department of Physics of Materials at the Universidad Complutense, Madrid, Spain in 1994–1996 as well as a research professor in QSRC at Dongguk University, Seoul, Korea in 2000–2008. His research interests are in the formation and characterization of multifunctional quantum structures and nanomaterials based on oxide multiferroics and graphene for use in photonic and electronic nano-information technologies and sustainable energy devices. He is member of the Expert Council of the Global Research Laboratory in the field of Nanoscience and Nanotechnology since 2006. He was Chairman of various sessions of International Conferences on Electronic and Optical Nanomaterials and Devices.

Olesya Kapitanova received the bachelor degree from Department of Materials Science, Moscow State University, Russia, in 2009. Olesya is now the second year master student of Department of Materials Science, Moscow State University. Her research interests are in the synthesis and characterization of oxide nanomaterials and structures for use in the fabrication of electronic and photonic nanodevices. In 2010 she was a researcher of the Quantum-functional Semiconductor Research Center at Dongguk University, Seoul, Korea.

Sang Wuk Lee received BS, MS, and Ph. D degrees in physics from Dongguk University of Seoul, Korea in 1996, 1998, and 2004, respectively. His research area is semiconductor materials and devices for optoelectronics and information displays. He developed Electroluminescence Lamps in ELK corporation in Daejon, Korea, and LED based on GaN in SanPlus corporation in Pyungtaek, Koea as a senior researcher. He is working for the growth and the applications of ZnO thin film and nanorods for optoelectronics since 2007 as a visiting professor of the Quantum-functional Semiconductor Research Center (QSRC) of Dongguk University, Seoul, Korea.

Andrey Nikolayevich Baranov received the Ph. D. degree in physical chemistry from Moscow State University, Russia, in 1990. He became an academic staff of Kurnakov Institute of General and Inorganic Chemistry in 1993 and worked on the synthesis of oxide functional materials. From 2003 to 2004, he stayed at Korea Institute of Science and Technology in Seoul, Republic of Korea. Since 2003, he has been working on the research of the synthesis of ZnO nanostructures and nanomaterials. He is currently a Leading Researcher of Chemistry Department of Lomonosov Moscow State University.

Tae Won Kang is a professor of Department of Physics at Dongguk University and also serves currently as the director of Quantum-Functional Semiconductor Research Center, Seoul, Korea. He received the Ph. D. degrees in physics from Dongguk University, Seoul, Korea in 1982 and the D. Eng. in semiconductor engineering from Osaka University, Osaka, Japan, in 2000. He has been an adjunct professor of University of Illinois at Chicago Circle, U.S.A. since 2006. He is a Fellow of the Korean Physical Society. His research activities include semiconductor nanodevices, self-assembly growth of quantum structures, molecular beam epitaxy and nanoepitaxy of heterostructures, spintronics materials and devices; electron spin and coherence properties of magnetic semiconductors, quantum structures for implementation of spin-based quantum information. He is currently working in the fields of diluted magnetic, ferroelectric and multiferroic semiconductors, LED and FED devices based on ZnO and GaN, RFID and printing electronics, energy harvest-wind-solar cells, graphene and topological insulators. He was the Chairman of Organizing Committee of the International Conference on Physics of Semiconductors (ICPS), July, 2010, Seoul, Korea; the Chairman of Organizing Committee of the 13th International Symposium on II–VI Compounds (September 2007, Jeju, Korea); the Chairman of Organizing Committee of the 13th International Symposium on Physics of Semiconductor and Applications (ISPSA), August 2006, Jeju, Korea.